Crystal structure phase transitions and a vibrational study of disordered $RbH(SO_4)_{0.81}(SeO_4)_{0.19}$ solid solution

1998 J. Phys.: Condens. Matter 10 8235

(http://iopscience.iop.org/0953-8984/10/37/010)

J. Phys.: Condens. Matter **10** (1998) 8235–8245. Printed in the UK PII: S0953-8984(98)94237-0

Crystal structure phase transitions and a vibrational study of disordered $RbH(SO_4)_{0.81}(SeO_4)_{0.19}$ solid solution

M Gargouri, R Ben Hassen, T Mhiri and A Daoud
Laboratoire de l'Etat Solide, Faculté des Sciences de Sfax, 3038 Sfax, Tunisia

Received 13 May 1998, in final form 14 July 1998

Abstract. $RbH(SO_4)_{0.81}(SeO_4)_{0.19}$ Mm = 189.58 single crystals were grown which appear to be different from $RbHSO_4$ and $RbHSeO_4$. The space group is monoclinic Cm, the lattice constants are $a = 14.916(3)$ Å, $b = 24.860(3)$ Å, $c = 4.6419(8)$ Å $b = 90.01(2)^\circ$, $V = 1721.3(5)$ Å^3, $Z = 16$, $Dx = 2.92$ g cm^{-3}, $\lambda(MoK_\alpha) = 0.710\,69$ Å, $\mu = 6.53$ cm^{-1}, $T = 293$ K (room-temperature phase), $R = 0.076$ and $wR2 = 0.174$ for 3450 observed reflections. The structure consists of five crystallographically independent molecules in the asymmetric unit. Each of the independent sulphate or selenate tetrahedron is linked to a translationally equivalent sulphate or selenate by acentrically ordered hydrogen bonds. The separated chains of asymmetric hydrogen bonds run parallel to the c-axis. The distance O–H. . .O varies between 2.48 Å and 2.60 Å.

1. Introduction

The rubidium sulphate $RbHSO_4$ has monoclinic structure with space group $P2_1/c$ and the rubidium selenate $RbHSeO_4$ has a triclinic unit cell $P1$. Their structures consist respectively of two and three crystallographically independent molecules in an asymmetric unit. Each of the independent sulphate or selenate tetrahedrons is linked to a translationally equivalent sulphate or selenate by acentrically ordered hydrogen bonds [1–6]. $RbHSO_4$ undergoes a second-order phase transition from a paraelectric to a ferroelectric phase at $T_c = 260$ K when $RbHSeO_4$ was shown to be ferroelectric below 370 K.

In the present study we have investigated mixed crystals of a new solid solution: $RbH(SO_4)_{0.81}(SeO_4)_{0.19}$, by means of x-ray diffraction, calorimetry, IR, Raman spectroscopy and complex impedance analysis. The structure determination and the transitional behaviour will be discussed and compared with homologous compounds.

2. Experimental details

2.1. Synthesis and characterization

Colourless single crystals of $RbH(SO_4)_{0.81}(SeO_4)_{0.19}$ were prepared by the reaction with stoichiometric quantities of Rb_2SO_4–H_2SO_4–H_2SeO_4 in water solution:

$$Rb_2SO_4 + (1-2x)H_2SO_4 + 2xH_2SeO_4 \rightarrow 2RbH(SO_4)_{1-x}(SeO_4)_x.$$

Single crystals were grown from water solution by slow evaporation at a constant temperature of 293 K†. The crystals had parallelepipedic form with a size of about

† The composition of the compound is confirmed by chemical analysis (service d'analyse du CNRS, 69 vernaison, France).

0953-8984/98/378235+11$19.50

$(2 \times 1 \times 0.5)$ mm^3. Infrared absorption spectra of suspensions of crystalline powders in KBr were recorded on a IR-470 Shymadzu spectrophotometer in the 400–4000 cm^{-1} region. Raman spectra of polycrystalline samples sealed in glass tubes were performed by employing a RTI Dilor instrument using the 514.5 nm of a spectra-physics argon ion laser. Differential scanning calorimetry (DSC) was performed with a DSC Mettler TA 4000 between 100 and 500 K. The electrical properties were determined by the complex impedance method using a frequency response analyser of Solartron 1260 type. The frequency range was 10^{-2}–10^6 Hz and measurements were carried out, under dry nitrogen, between 300 and 450 K for several temperature cycles.

2.2. Crystallographic data

A small specimen of parallelipipedic shape $(0.60 \times 0.30 \times 0.10)$ mm^3 was selected for x-ray diffraction. Data collection was performed with an Enraf-Nonius CAD-4 diffractometer, using MoKα radiation; $\omega-2\theta$ scans were used. The counter slight width was $\theta_{max} = 25.95^\circ$; 2058 reflections with Miller indices $-18 \leqslant h \leqslant 18$, $-30 \leqslant k \leqslant 0$ and $-5 \leqslant l \leqslant 5$ were collected. The space group is Cm from the systematic extinctions. The positions of the Rb, S and Se atoms were found from a three-dimensional Patterson map. Atomic scattering factors for Rb, S, Se, O and H were taken from international tables for x-ray crystallography [7, 8]. The function minimized by the full-matrix least squares analysis on F^2 was $\Sigma\omega(|F_0|^2-|F_C|^2)$. The final discrepancy factors were $R = 0.076$ and $wR2 = 0.174$ (poor quality of crystal) and a goodness of fit $s = 1.003$ for 2058 unique reflections was obtained. Refinement with anisotropic thermal parameters gives for all atoms a weighting scheme

$$W = \frac{1}{\sigma^2(F_0^2) + (0.0692P)^2 + 154.6836P}$$

where $P = (F_0^2 + 2F_c^2)/3$.

The isotropic extinction coefficient is $g = 0.000\,65$. The final positional and thermal parameters are given in table 1.

3. Results and discussion

3.1. X-ray diffraction study

The final atomic coordinates and the anisotropic parameters are given in tables 1 and 3. The bond distances and angles are listed in table 2. From figure 1 it is easily shown that the crystal is built up from separate chains of hydrogen-bonded sulphate (selenate) ions. These chains run parallel to the c-axis. This structure of $RbH(SO_4)_{0.81}(SeO_4)_{0.19}$ consists of five non-equivalent tetrahedra AO_4^{2-} (A = S, Se) which are different from those of pure compound $RbHSO_4$ and $RbHSeO_4$ [1, 3].

The AO_4^{2-} tetrahedron is distorted, with distances A–O in the range 1.46–1.60 Å. The hydrogen bonds are asymmetric as in the case of $RbHSO_4$ and $RbHSeO_4$ [1, 3]. The values of the distance O–H. . .O are situated in three groups, in the vicinity of 2.45 Å, 2.53 Å and 2.58 Å.

These observations are in agreement with the distance of the A–O acceptor (table 2).

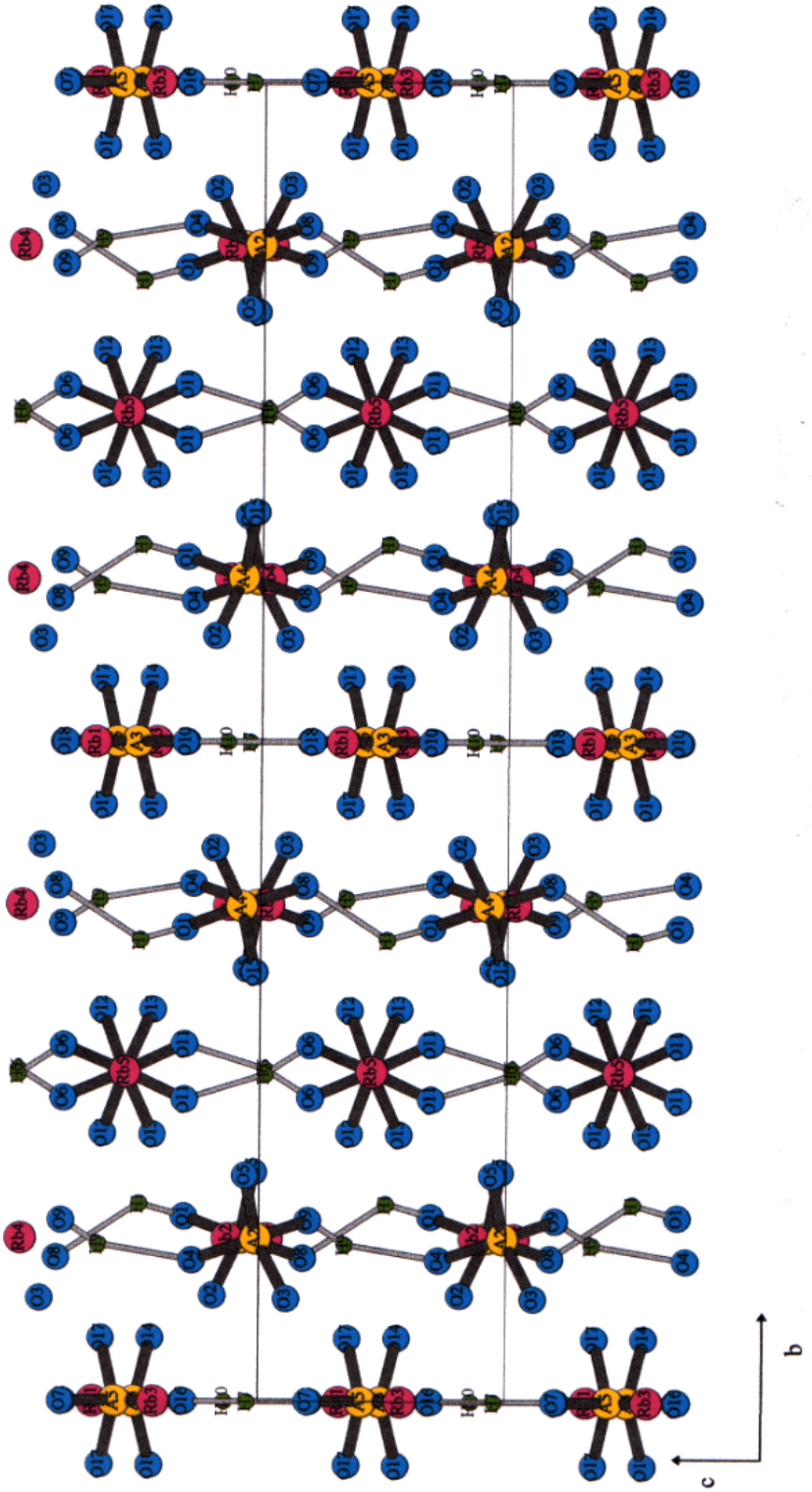

Figure 1. Projection of the $RbH(SO_4)_{0.81}(SeO_4)_{0.19}$ crystal structure on the *bc* plane.
(This figure can be viewed in colour in the electronic version of the article; see http://www.iop.org)

Table 1. Atomic and equivalent isotropic displacement parameters (in Å) for $RbH(SO_4)_{0.81}(SeO_4)_{0.19}$. U_{eq} is defined as one-third of the trace of the orthogonolized U_{ij} tensor.

Atom	Multiplicity	*x*	*y*	*z*	U_{eq}
Rb(1)	1	0.4180(3)	0.0000	0.1711(8)	0.0297(9)
Rb(2)	1	0.6249(2)	0.123 58(11)	0.6275(6)	0.0345(9)
Rb(3)	1	0.9181(3)	0.0000	0.9243(8)	0.0318(10)
Rb(4)	1	0.1246(2)	0.123 54(11)	0.4676(6)	0.0355(9)
Rb(5)	1	0.4220(3)	0.250 17(15)	1.0459(12)	0.0452(8)
Se(1)	0.362(19)	0.6673(4)	0.2501(2)	1.0473(17)	0.0312(16)
S(1)	0.638(19)	0.6673(4)	0.2501(2)	1.0473(17)	0.0312(16)
Se(2)	0.13(2)	0.8807(4)	−0.1237(2)	0.5135(12)	0.0144(18)
S(2)	0.87(2)	0.8807(4)	−0.1237(2)	0.5135(12)	0.0144(18)
Se(3)	0.04(3)	1.1602(7)	0.0000	1.0025(18)	0.037(4)
S(3)	0.96(3)	1.1602(7)	0.0000	1.0025(18)	0.037(4)
Se(4)	0.18(2)	0.3802(5)	0.124 41(18)	0.5760(14)	0.022(2)
S(4)	0.82(2)	0.3802(5)	0.124 41(18)	0.5760(14)	0.022(2)
Se(5)	0.04(6)	0.6606(10)	0.0000	1.084(3)	0.038(5)
S(5)	0.96(6)	0.6606(10)	0.0000	1.084(3)	0.038(5)
O(1)	1	0.306(2)	0.1407(12)	0.807(5)	0.069(9)
O(2)	1	0.4326(13)	0.0806(9)	0.686(5)	0.033(5)
O(3)	1	0.9342(14)	−0.0782(9)	0.389(4)	0.030(5)
O(4)	1	0.8276(15)	−0.1072(9)	0.774(4)	0.036(5)
O(5)	1	0.9384(14)	−0.1716(9)	0.558(6)	0.047(6)
O(6)	1	0.7257(14)	0.2699(9)	1.295(4)	0.034(5)
O(7)	1	0.740(2)	0.0000	1.299(8)	0.067(12)
O(8)	1	0.3277(19)	0.1089(13)	0.322(4)	0.074(9)
O(9)	1	0.7980(16)	−0.1374(9)	0.302(5)	0.041(5)
O(10)	1	1.2430(17)	0.0000	0.810(6)	0.037(8)
O(11)	1	0.7322(15)	0.2290(8)	0.806(4)	0.035(5)
O(12)	1	0.6150(16)	0.2031(8)	1.135(5)	0.039(5)
O(13)	1	0.6109(8)	0.2973(8)	0.933(5)	0.045(6)
O(14)	1	1.1053(17)	0.0482(8)	0.937(6)	0.052(7)
O(15)	1	0.435(2)	0.1745(10)	0.525(7)	0.065(8)
O(16)	1	0.692(3)	0.0000	0.805(9)	0.066(12)
O(17)	1	0.613(2)	−0.0487(9)	1.141(6)	0.058(7)
O(18)	1	1.198(4)	0.0000	1.294(7)	0.12(2)
H(1)	1	0.337 95	0.150 60	0.987 86	
H(9)	1	0.802 23	0.880 68	0.152 60	
H(10)	1	1.224 59	0.0000	0.639 42	
H(7)	1	0.737 21	0.0000	0.505 06	
H(6)	1	0.722 84	0.248 26	0.779 00	

3.2. Vibrational study

Raman spectra of polycrystalline samples of $RbH(SO_4)_{0.81}(SeO_4)_{0.19}$ have been recorded in the spectra ranges 10–1300 cm^{-1}, see table 4. We shall not give a detailed assignment here but we try to identify some external and internal modes. Figures 2 and 3 and table 4 show Raman and IR spectra of the mixed compound $RbH(SO_4)_{0.81}(SeO_4)_{0.19}$. The frequency Raman spectrum of $RbH(SO_4)_{0.81}(SeO_4)_{0.19}$ is characterized by the presence of external and internal bands identified by analogy with $RbHSO_4$ and $RbHSeO_4$ pure compounds and previous works on this family of compounds [9–16]. The external vibrational bands at 37, 40 and 55 cm^{-1} are assigned to translational vibrations of Rb^+ ions while the 75, 90, 103,

Table 2. Selected bond length (in Å) and angles (°) (A = S, Se).

Bond length (Å)		Angle (°)	
A(1)–O(12)	1.46(2)	O(12)–A(1)–O(6)	110.6(14)
A(1)–O(6)	1.52(2)	O(12)–A(1)–O(13)	114.4(14)
A(1)–O(13)	1.54(2)	O(6)–A(1)–O(13)	109.0(13)
A(1)–O(11)	1.57(2)	O(12)–A(1)–O(11)	105.1(13)
A(2)–O(5)	1.48(2)	O(6)–A(1)–O(11)	107.1(12)
A(2)–O(3)	1.50(2)	O(13)–A(1)–O(11)	110.2(13)
A(2)–O(4)	1.50(2)	O(5)–A(2)–O(3)	110.6(13)
A(2)–O(9)	1.61(3)	O(5)–A(2)–O(4)	114.3(13)
A(3)–O(18)	1.48(2)	O(3)–A(2)–O(4)	112.6(12)
A(3)–O(14)	1.48(2)	O(5)–A(2)–O(9)	111.1(13)
A(3)–O(14)	1.48(2)	O(3)–A(2)–O(9)	109.3(12)
A(3)–O(10)	1.52(3)	O(4)–A(2)–O(9)	98.2(12)
A(4)–O(2)	1.434(19)	O(18)–A(3)–O(14)	113.7(15)2
A(4)–O(8)	1.47(3)	O(18)–A(3)–O(14)	113.7(15)
A(4)–O(15)	1.51(3)	O(14)–A(3)–O(14)	108(2)2
A(4)–O(1)	1.60(3)	O(18)–A(3)–O(10)	103(2)
A(5)–O(16)	1.37(5)	O(14)–A(3)–O(10)	109.1(12)2
A(5)–O(17)	1.43(3)	O(14)–A(3)–O(10)	109.1(12)2
A(5)–O(17)	1.43(3)	O(2)–A(4)–O(8)	112.1(15)
A(5)–O(7)	1.55(3)	O(8)–A(4)–O(15)	112.6(15)
O(1)–H(1)...O(8)[a]	2.5365	O(8)–A(4)–O(15)	112.4(18)
O(9)–H(9)...O(4)[b]	2.6004	O(2)–A(4)–O(1)	109.6(14)
O(10)–H(10)...O(18)[b]	2.4815	O(8)–A(4)–O(1)	103.5(15)
O(7)–H(7)...O(16)[a]	2.4533	O(15)–A(4)–O(1)	105.9(17)
O(6)–H(6)...O(11)[a]	2.5867	O(16)–A(5)–O(17)	110.0(16)
O(1)–H(1)	0.9981	O(16)–A(5)–O(17)	110.0(16)
H(1)...O(8)	1.8694	O(17)–A(5)–O(17)	116(3)
O(9)–H(9)	0.8278	O(16)–A(5)–O(7)	111(2)
H(9)...O(9)	1.8234	O(17)–A(5)–O(7)	105.3(13)
O(10)–H(10)	0.8373	O(17)–A(5)–O(7)	105.3(13)2
H(10)...O(18)	0.9651	O(1)–H(1)...O(8)	121.37
O(7)–H(7)	1.6471	O(9)–H(9)...O(4)	155.72
H(7)...O(16)	1.5377	O(10)–H(10)...O(18)	174.14
O(6)–H(6)	1.0122	O(7)–H(7)...O(16)	156.55
H(6)...O(11)	1.5996	O(6)–H(6)...O(11)	163.67

[a] Symmetry, $x, y, z + 1$.
[b] Symmetry, $x, y, z - 1$.

108 and 112 cm^{-1} bands involve librational and translational modes of $[HS(Se)O_4]^-$ anions (table 4 and figure 2(a)).

$RbH(SO_4)_{0.81}(SeO_4)_{0.19}$ is more disordered than pure compounds: $RbHSeO_4$, $RbHSO_4$. This disorder is evidenced by broadening of the T(Rb^+) modes near 37 and 40 cm^{-1}. The internal vibrational bands are approximately the superposition of those of $RbHSO_4$ and $RbHSeO_4$ as observed for $CsH(SO_4)_{0.76}(SeO_4)_{0.24}$ compounds [9]. In the Raman spectrum the bending bands in the 300–380 cm^{-1} range are assigned to ν_4 and ν_2 of the tetrahedral SeO_4 group. On the other hand, the bands observed in the region 400–600 cm^{-1} (figure 2(b)) are assigned to ν_4 and ν_2 of the SO_4 tetrahedral group. Alternatively, the 844(728) cm^{-1} bands can be interpreted as S(Se)–(OH) donor modes of the –S(Se)–O...HO–S(Se)– hydrogen bonded system (table 4). The presence of five peaks grouped in two bands at 1043, 1019 cm^{-1} and 882, 870 cm^{-1} can be interpreted as S–O and Se–O acceptor modes, respectively.

Table 3. Anisotropic displacement parameters (in 10^{-3} Å^2). The anisotropic displacement exponent takes the form $(-2\pi^2[h^2a^{*2}U_{11} + \cdots + 2hka^*b^*U_{12}])$.

Atom	U_{11}	U_{22}	U_{33}	U_{23}	U_{13}	U_{12}
Rb(1)	0.033(2)	0.034(2)	0.0220(16)	0.000	0.0021(14)	0.000
Rb(2)	0.0302(16)	0.0325(16)	0.0406(19)	−0.0036(13)	−0.0014(13)	−0.0013(12)
Rb(3)	0.048(3)	0.025(2)	0.0225(17)	0.000	0.000	0.000
Rb(4)	0.0398(17)	0.0242(14)	0.0366(19)	0.0026(12)	−0.0034(13)	0.0001(12)
Rb(5)	0.0344(16)	0.0321(14)	0.0692(19)	0.0027(14)	0.0001(13)	−0.0029(11)
Se(1)	0.030(3)	0.041(3)	0.022(2)	−0.0048(18)	−0.0003(17)	−0.018(2)
S(1)	0.030(3)	0.041(3)	0.022(2)	−0.0048(18)	−0.0003(17)	−0.018(2)
Se(2)	0.015(3)	0.016(3)	0.012(3)	0.0069(17)	0.002(2)	0.0115(19)
S(2)	0.015(3)	0.016(3)	0.012(3)	0.0069(17)	0.002(2)	0.0115(19)
Se(3)	0.028(6)	0.082(9)	0.001(5)	0.000	−0.003(4)	0.000
S(3)	0.028(6)	0.082(9)	0.001(5)	0.000	−0.003(4)	0.000
Se(4)	0.035(4)	0.007(2)	0.025(3)	0.0042(18)	0.002(2)	0.019(2)
S(4)	0.035(4)	0.023(10)	0.025(3)	0.0042(18)	0.002(2)	0.019(2)
Se(5)	0.065(9)	0.023(10)	0.027(7)	0.000	−0.005(5)	0.000
S(5)	0.065(9)	0.023(10)	0.027(7)	0.000	−0.005(5)	0.000
O(1)	0.10(2)	0.085(19)	0.022(10)	0.019(11)	0.021(12)	0.036(17)
O(2)	0.010(9)	0.052(13)	0.037(10)	0.018(10)	−0.002(7)	0.021(9)
O(3)	0.026(10)	0.045(12)	0.020(8)	−0.010(8)	0.014(7)	−0.020(9)
O(4)	0.054(13)	0.036(11)	0.019(8)	0.005(8)	−0.005(8)	0.017(10)
O(5)	0.020(10)	0.039(12)	0.082(15)	0.025(12)	−0.006(10)	0.001(9)
O(6)	0.035(12)	0.041(12)	0.026(9)	−0.002(8)	−0.001(8)	−0.023(10)
O(7)	0.029(19)	0.13(4)	0.042(19)	0.000	−0.024(15)	0.000
O(8)	0.077(18)	0.13(2)	0.015(9)	0.000(11)	.0003(10)	0.081(17)
O(9)	0.033(11)	0.052(13)	0.036(10)	0.015(9)	0.009(8)	−0.021(9)
O(10)	0.000(11)	0.082(2)	0.031(14)	0.000	−0.006(9)	0.000
O(11)	0.040(12)	0.021(10)	0.044(10)	−0.012(8)	−0.006(9)	−0.003(9)
O(12)	0.027(11)	0.021(10)	0.068(14)	0.013(10)	0.000(9)	0.006(9)
O(13)	0.072(17)	0.018(9)	0.046(12)	0.009(9)	0.010(10)	−0.014(10)
O(14)	0.063(17)	0.018(10)	0.077(16)	−0.001(10)	0.006(12)	0.010(10)
O(15)	0.062(17)	0.046(14)	0.089(18)	0.021(14)	−0.013(14)	−0.013(12)
O(16)	0.10(3)	0.007(15)	0.09(3)	0.000	−0.01(2)	0.000
O(17)	0.068(18)	0.034(13)	0.072(15)	0.0014(12)	−0.038(13)	−0.021(12)
O(18)	0.11(4)	0.22(7)	0.016(16)	0.000	0.01(2)	0.000

In previous works [9–16] the splitting $\Delta\nu_A = \nu$(A–O)$-\nu$(A–OH) was used to discriminate between $(HAO_4^-)_n$ chains and $(HAO_4^-)_2$ dimers; when $\Delta\nu_A < 160$ cm^{-1}, the AO_4^{2-} ions are associated in $(HAO_4^-)_n$ chains. The x-ray diffraction results concerning the structure of $RbH(SO_4)_{0.81}(SeO_4)_{0.19}$ suggest that the room-temperature phase consists of $(HAO_4^-)_n$ chains. However, the values of $\Delta\nu_S = 195$, 171 cm^{-1} were superior to 160 cm^{-1}; this can be explained by the convolution between the chain translational vibrations with ν(S–O) bands. These perturbations can be the cause of the displacement of the frequency of ν(S–O) near 1043 and 1019 cm^{-1}. The splitting ($\Delta\nu_{Se} = 154$, 142 cm^{-1}) confirms this point of view.

3.3. Phase transitions

The results of the calorimetric study are presented in figure 4 which shows the results of heating of freshly prepared samples. Five distinct endothermal peaks are present at 245, 288, 353, 380 and 503 K. The calculated enthalpy at the first transition $T_{I-II} = 245$ K

Table 4. Infrared and Raman frequencies of $RbH(SO_4)_{0.8}(SeO_4)_{0.2}$. Internal and external vibrations (10/1300 cm^{-1}) at room temperature.

IR	I	Raman	I	Assignment
		17	w	
		20	w	
		37	s	
		40	s	$T(Rb^+)$
		45	w	
		55	m	
		61	m	
		75	s	
		81	w	$R,T(HAO_4^-)$
		90	s	
		95	m	
		103	m	
		108	w	
		112	w	
		310	s	
		335	s	ν_2(Se–O)
472	m	385	sh	
492	w	404	vs	ν_4(Se–O)
532	w	420	m	ν_2(S–O)
		444	vs	
588	vs	581	vs	
644	w	595	m	ν_4(S–O)
672	w	609	vs	
696	w			
720	m	728	vs	ν(Se–OH) donnor
760	w	848	sh	ν(S–OH) donnor
872	vs	870	vs	ν(Se–O) acceptor
883	sh	882	vs	ν(Se–O) acceptor
920	vs	917	w	
		938	w	
		974	w	ν_3(Se–O)
1020	sh	1019	vs	
1045	vs	1043	vs	ν(S–O) acceptor
1112	vs			ν(S–O) acceptor
1176	sh			
1200	sh	1196	w	
1208	vs			
1248	sh			

vs: very strong, s: strong, m: medium, w: weak, sh: shoulder.

was $\Delta H = 0.129$ cal g^{-1} and for the second transition $T_{II-III} = 288$ K it was $\Delta H = 0.267$ cal g^{-1}. By comparison with $CsH(SO_4)_{0.76}(SeO_4)_{0.24}$ [9], the endothermal peak with maxima at about 353 K with enthalpy values 1.088 cal g^{-1} characterizes the conversion of infinite chains $(HAO_4^-)_n$ into cyclic dimers $(HAO_4^-)_2$. The temperature of the superionic phase transition (SPT) observed at 455 K under pressure and 446 K for $RbHSO_4$ and $RbHSeO_4$ respectively (table 5) [5, 6], presents a decreasing from that for our material which appears at 380 K with $\Delta H = 0.23$ cal g^{-1}. The last transition at $T_M = 482$ K

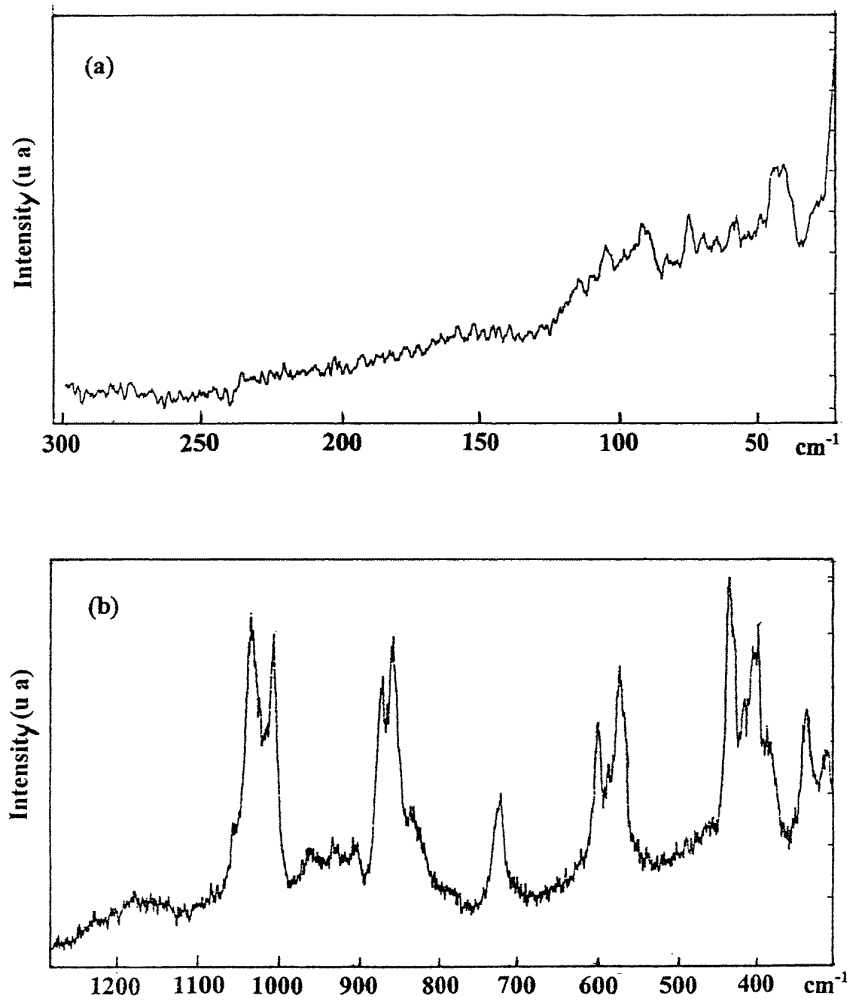

Figure 2. Raman spectra at room temperature for $RbH(SO_4)_{0.81}(SeO_4)_{0.19}$.

corresponds to the molten state. This result is consist with the disordered phase IV in the case of the new solid solution $RbH(SO_4)_{0.81}(SeO_4)_{0.19}$ rather than with those for $RbHSeO_4$ and $RbHSO_4$ under pressure. The temperature dependence of the conductivity between 300 and 450 K is given in figure 5 as a plot of $\log \sigma T$ against inverse temperature: an arrhenius-type behaviour, $\sigma T = \sigma_0 \exp(-\Delta E\sigma/kT)$, is shown on both sides of a transition temperature T_{tr} ($\cong$370 K) close to the IV–V transition. The conductivity data, represented in figure 5 and collected in table 6, correspond to the second heating run of $RbH(SO_4)_{0.81}(SeO_4)_{0.19}$.

4. Conclusion

The results of x-ray diffraction, vibrational spectroscopy, calorimetric and electrical measurements against temperature show that $RbH(SO_4)_{0.81}(SeO_4)_{0.19}$ crystals undergo a superionic phase transition at 380 K related to the motion of rapid $[HS(Se)O_4]^-$ reorientation

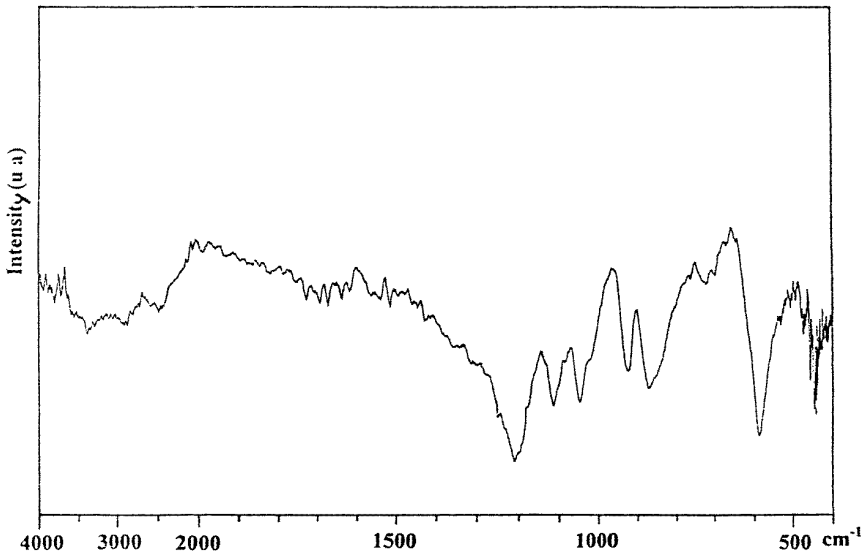

Figure 3. IR spectra at room temperature for $RbH(SO_4)_{0.81}(SeO_4)_{0.19}$.

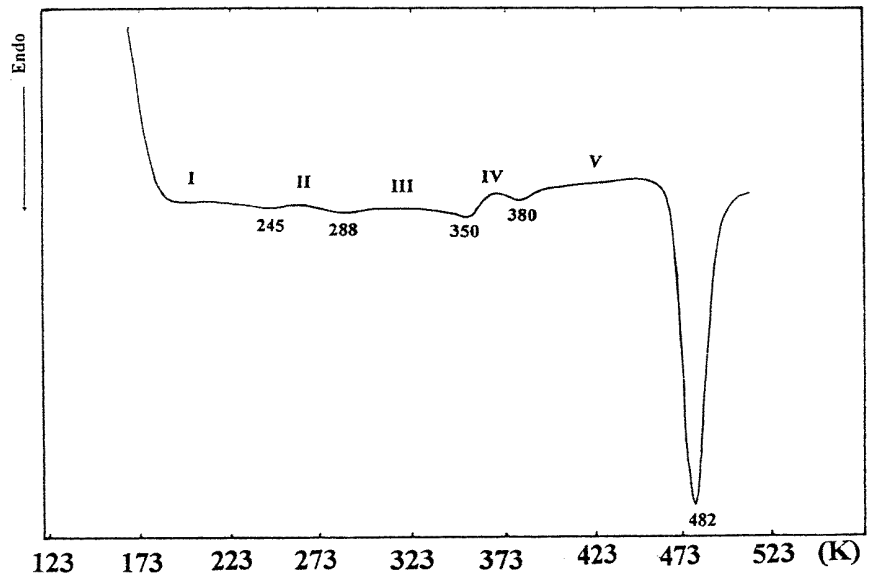

Figure 4. Differential scanning calorimetry of $RbH(SO_4)_{0.81}(SeO_4)_{0.19}$ between 100 K and 500 K.

and fast H^+ diffusion. The new title compounds exhibit both protonic and ionic conductivity, as in pure compounds $RbHSeO_4$ [6].

The presence of a ferroelectric transition in $RbHSO_4$ and $RbHSeO_4$ [5, 6] suggests that the presence of a ferroelectric transition for the new solid solution $RbH(SO_4)_{0.81}(SeO_4)_{0.19}$ can explain the increasing value of the final discrepancy factor R.

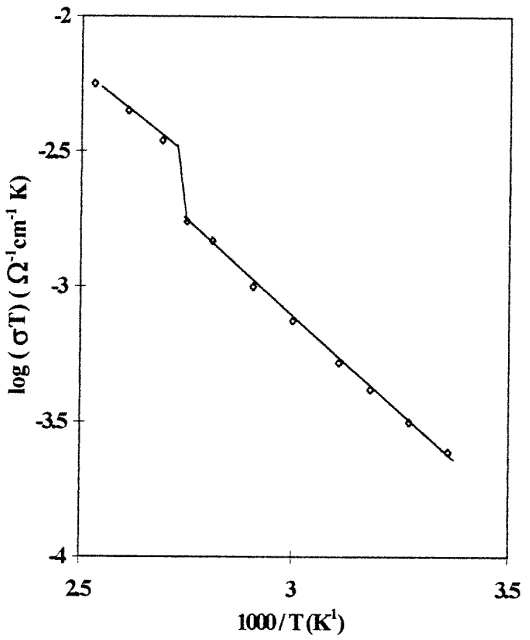

Figure 5. The temperature dependence of $\log \sigma T$ for $RbH(SO_4)_{0.81}(SeO_4)_{0.19}$ at various temperatures for the second heating.

Table 5. Representation of the relationship for $RbHSO_4$, $RbHSeO_4$ and $RbH(SO_4)_{0.81}(SeO_4)_{0.19}$.

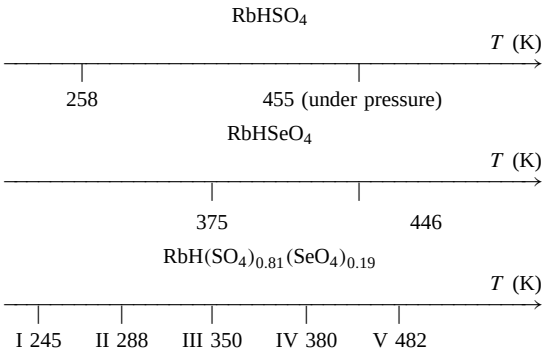

Table 6. Conductivity and activation energies of $RbH(SO_4)_{0.81}(SeO_4)_{0.19}$.

Temperature	313 K	300–380 K	453 K
	$\sigma(\Omega^{-1}\ cm^{-1})$	ΔE_σ(eV)	$\sigma(\Omega^{-1}\ cm^{-1})$
M_2	2.1×10^{-6}	0.29	7×10^{-4}

M_2 second heating.

Acknowledgment

We are grateful to Dr A Driss for granting access to the CAD4 diffractometer.

References

[1] Barn J and Lis T 1987 *Acta Crystallogr.* C **43** 811
[2] Ashmore J P and Petch H E 1982 *Phys. Rev.* B **26** 5897
[3] Waskowska A, Olejnik S and Lukaszewiz K 1978 *Acta Crystallogr.* B **34** 3334
[4] Tsukamata T 1984 *Japan. J. Appl. Phys.* **4** 424
[5] Ashmore J P and Petch H E 1975 *Cass. J. Phys.* **53** 2694
[6] Tsukamoto T, Komukae M, Suzuki Sh, Futama H and Makita Y 1983 *J. Phys. Soc. Japan* **52** 3966
[7] Scheldtrick G M 1990 *Shelx S-86. Program for the Solution of Crystal Structures* University of Gattingen, Germany
[8] Scheldtrick G M *Shelx L-93. Program for Crystal Structure Determination*
[9] Gargouri M, Mhiri T, Daoud A and Jouini T 1997 *Phys. Status Solidi* b **200** 3
[10] Toupry N, Poulet H and Le Postollec M 1981 *J. Raman, Spectrosc.* **11** 2
[11] Goypiron A, de Villepin J and Novak A 1980 *J. Raman Spectrosc.* **9** 297
[12] Gargouri M, Mhiri T and Daoud A 1997 *J. Phys.: Condens. Matter* **9** 10 977
[13] Torrie B M, Lin C C, Binberk O S and Anderson A 1972 *J. Phys. Chem. Solids Chem.* **33** 697
[14] Kettpe S F A, Jayassoriya U A and Norby L J 1984 *J. Phys. Chem. Solids* **88** 5971
[15] Bazhulin P A, Mysaswi T P and Rakov A V 1964 *Sov. Phys.–Solid State* **5** 1299
[16] Gargouri M, Mhiri T, Reau J M, Senegas J and Daoud A 1997 *Solid State Ionics* **100** 225